Annals of Botany **82**: 203–212, 1998

Characterization of the Light Environment in Canopies Using 3D Digitising and Image Processing

H. SINOQUET*, S. THANISAWANYANGKURA*†, H. MABROUK‡ and P. KASEMSAP§

** INRA-PIAF, Domaine de Crouelle, 63039 Clermont-Ferrand Cedex 02, France, † Department of Botany, Faculty of Sciences, Kasetsart University, Bangkok, Thailand, ‡ INRA-Viticulture, 2 Place Viala, 34060 Montpellier Cedex 1, France and § Department of Agronomy, Faculty of Agriculture, Kasetsart University, Bangkok, Thailand*

Received: 12 January 1998 Returned for revision: 25 February 1998 Accepted: 26 April 1998

A method to measure light interception by vegetation canopies is presented which uses a 3D digitiser and image processing software. The 3D digitiser allows for simultaneous acquisition of the spatial co-ordinates of leaf locations and orientations. Software for image synthesis is used to make virtual photographs of the real canopy. Information on light interception is derived from the virtual images by using simple features of image analysis software. The method is applied to cotton, grapevine and young mango plants. Calculations are made of light interception at the canopy level, light partitioning between plant organs, vertical profiles of light interception, fisheye photographs and leaf irradiance distribution.

Key words: 3D digitising, image analysis, light interception, *Gossypium hirsutum* L. *Vitis vinifera* L., *Mangifera indica* L., cotton, grapevine, mango, canopy.

INTRODUCTION

Interactions between light and vegetation have been widely studied because of their implications for plant ecophysiology and remote sensing. The geometrical structure of the vegetation canopy, i.e. the location, shape and orientation of the plant elements (Ross, 1981) and the optical properties of the plant elements determine the light distribution in the canopy. Light distribution within the canopy influences a large number of physiological functions (e.g. photosynthesis, transpiration, stomatal aperture), and particularly photomorphogenesis which is involved in the dynamics of development of plant geometry.

Methods for the measurement of canopy geometry may involve direct measurement of the location and orientation of the plant elements, or geometric parameters may be inferred from radiation measurements using photographs or light sensors. Of the direct methods, three-dimensional (3D) digitising of foliage canopies consists of measuring spatial co-ordinates (x, y, z) of plant parts (Lang, 1973). Three-dimensional digitising is presently the most powerful direct method for plant geometry measurement because: (1) it can be applied at the leaf scale; and (2) it may be combined with the measurement of other plant element attributes e.g. plant topology (Sinoquet and Rivet, 1997). Three-dimensional digitising has involved various techniques: articulated arms (Lang, 1973), sound propagation (Sinoquet, Moulia and Bonhomme, 1991; Room, Hanan and Prusinkiewicz, 1996) and current induction in magnetic fields (Moulia and Sinoquet, 1993; Smith and Curtis, 1995; Sinoquet and Rivet, 1997; Thanisawanyangkura *et al*., 1997). The latter is presently the most convenient because: (1) unlike the sonic digitiser, it is insensitive to masking and to wind and temperature fluctuations, thus it may be used in the field; (2) unlike articulated arms, the pointer is not cumbersome; (3) the measurement volume is the largest; and (4) it measures not only spatial co-ordinates but also surface orientation.

Methods for measuring the light microclimate have become very common. However, difficulties remain when investigating light distribution in canopies, namely in terms of light partitioning between several vegetation components, e.g. intercropping, (Sinoquet and Caldwell, 1995) or of irradiance at particular leaves. For these purposes, the only way to measure directly is to fix small sensors onto leaf surfaces (Gutschick *et al*., 1985; Roden and Pearcy, 1993) although reliable sampling strategies need to be better defined and probably require a large number of sensors (Sinoquet *et al*., 1997).

An alternative approach consists of deriving attributes of the light microclimate from 3D plant models and computer graphics (Meyer *et al*., 1984; Buwalda, Curtis and Smith, 1993; Chen *et al*., 1993). In this paper, we propose a method to construct 3D plant models from 3D digitising. Commercial software is used to create virtual photographs from 3D simulations of the digitised plants. Image processing of the virtual photographs allows information on the light distribution in the canopy to be derived. Applications of the method to light partitioning between vegetation components and the distribution of leaf irradiance is illustrated using cotton (*Gossypium hirsutum* L.), grapevine (*Vitis vinifera* L.) and young mango (*Mangifera indica* L.) plants as examples.

0305-7364/98/080203 + 10 $30.00/0 bo980665

MATERIALS AND METHODS

Canopy structure

3D digitiser. Leaf location and orientation were measured using an electromagnetic 3D digitiser (Fastrak, Polhemus Inc., Cochester, VT, USA). The device consists of a pointer which looks like a small PC mouse and houses three electromagnetic coils. When supplied with alternating current low frequency magnetic fields are generated from the coils (Polhemus, 1993). When the pointer is located at a particular position in the magnetic fields the induced currents are related to the spatial co-ordinates (Raab *et al*., 1979).

Orientation angles measured by the digitiser are Euler angles, i.e. a set of three angles of rotation (Fig. 1). The first angle is the azimuth angle, Φ, i.e. a rotation around the vertical axis z. The azimuth rotation makes the reference moving from (x, y, z) to (x_1, y_1, z). The second angle is an inclination angle, α, i.e. a rotation around axis y_1. The inclination rotation makes the reference moving from (x_1, y_1, z) to (x_2, y_1, z_1). The third angle is a twist angle, θ, i.e. a rotation around axis x_2. After the third rotation, the reference is that of the pointer.

The digitiser error in measuring spatial co-ordinates is less than 1 mm when used in controlled conditions (Moulia and Sinoquet, 1993). In the field, the error is about 1 cm, because of plant movements due to wind and operator effects (Thanisawanyangkura *et al*., 1997).

Foliage digitising. The spatial co-ordinates and the orientation of each leaf were measured from a single digitising record. The digitised point was the junction between petiole and lamina. The pointer was held parallel to the leaf blade with the pointer axis (i.e. axis x_2 in Fig. 1) parallel to the leaf midrib. Thus measured azimuth, Φ, and inclination, α, were midrib azimuth and inclination, respectively. Measured angle, θ, was the twist angle of the leaf blade around the midrib.

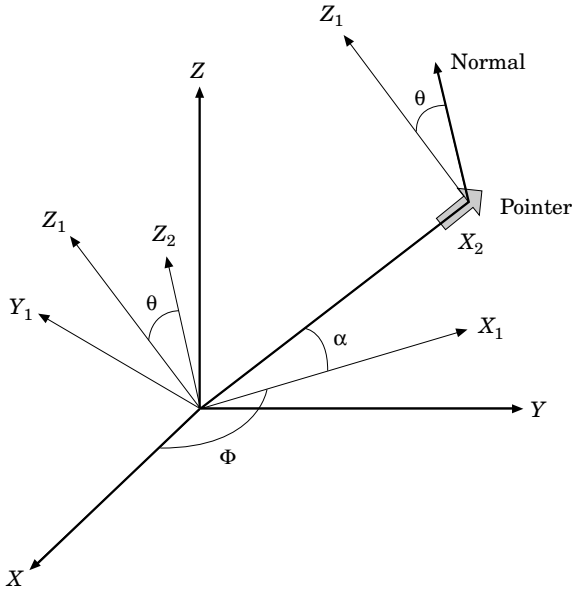

FIG. 1. Euler angles as measured by the 3D digitiser: azimuth angle Φ, i.e. a rotation around the vertical axis z; inclination angle α, i.e. a rotation arond axis y_1; twist angle θ, i.e. a rotation around axis x_2.

At the same time as the digitising process, leaf length and width were measured with a ruler. The digitiser was not used to measure leaf dimensions because of the 1 cm-error when locating a point in the field. Other leaf attributes may also be recorded at the same time. For each leaf, blade area was estimated from leaf dimensions using an allometric relationship.

This method allows one to obtain a description of the 3D plant geometry at the leaf scale, where location, orientation, blade area and possibly other attributes of each leaf are recorded.

Digitised plants. Cotton ('DES 119') was planted at the Department of Agronomy, Faculty of Agriculture, Kasetsart University, Kamphaengsaen Campus, Nakhon Pathom, Thailand (14·02° N, 99·97° E), on 12 Feb. 1997, in rows with north-south orientation of 0·80 m spacing and between-plant spacing of 0·25 m. Leaf digitising was carried out on five consecutive plants in the same row, 65 d after planting when the leaf area index (LAI) was 3·05. At this stage, mean leaf number per plant was 85 and mean plant height was about 1 m. During digitising, leaves attached to the main stem, vegetative branches and fruiting branches, were distinguished. Leaf area was estimated from an allometric relationship between midrib length (L) and leaf blade area (A) measured by a leaf area meter (Li-Cor 3100, Li-Cor Inc., Lincoln, NE, USA), with: $A = 0{\cdot}946\ L^2$, $r^2 = 0{\cdot}92$, $n = 225$.

The structure of the grapevine canopy was digitised on one 15-year-old Merlot plant (on SO4 rootstock) trained to a vertical trellis in the experimental vineyard of the Ecole Nationale Supérieure Agronomique, Montpellier, France, in August 1996. Row and plant spacings were 2·5 and 1·2 m, respectively. Row orientation was east-south-east/west-north-west. At the time of measurement, the grapevines had completed their vegetative growth. Plant height and width were about 1·8 and 0·5 m, respectively, and the plant had 562 leaves. During digitising, primary and lateral leaves, i.e. leaves attached to the primary and lateral shoots, respectively, were distinguished. The relationship between midrib length, L, and blade area, A, measured with a leaf area meter CID 203 (CID Inc., WA, USA) was: $A = 1{\cdot}26\ L^2$, $r^2 = 0{\cdot}97$, $n = 165$.

The mango canopy was analysed at the Department of Agronomy, Faculty of Agriculture, Kasetsart University, Kamphaengsaen Campus, Nakhon Pathom, Thailand, on 19 Apr. 1997. A 1-year-old mango ('Chok Anan') plant having six flushes and 168 leaves was digitised. The relationship between leaf length L and width W, and blade area A measured with a leaf area meter (Li-Cor 3100) was: $A = 0{\cdot}77\ LW$, $r^2 = 0{\cdot}95$, $n = 75$.

Plant image synthesis

Virtual photographs of digitised plants were created using a soft programme (freeware POV-Ray, Persistence of Vision Raytracer, version 3.01). POV-Ray is a ray-tracing software devoted to image synthesis, which allows definition of the elements of a scene from numerous shapes, as well as from

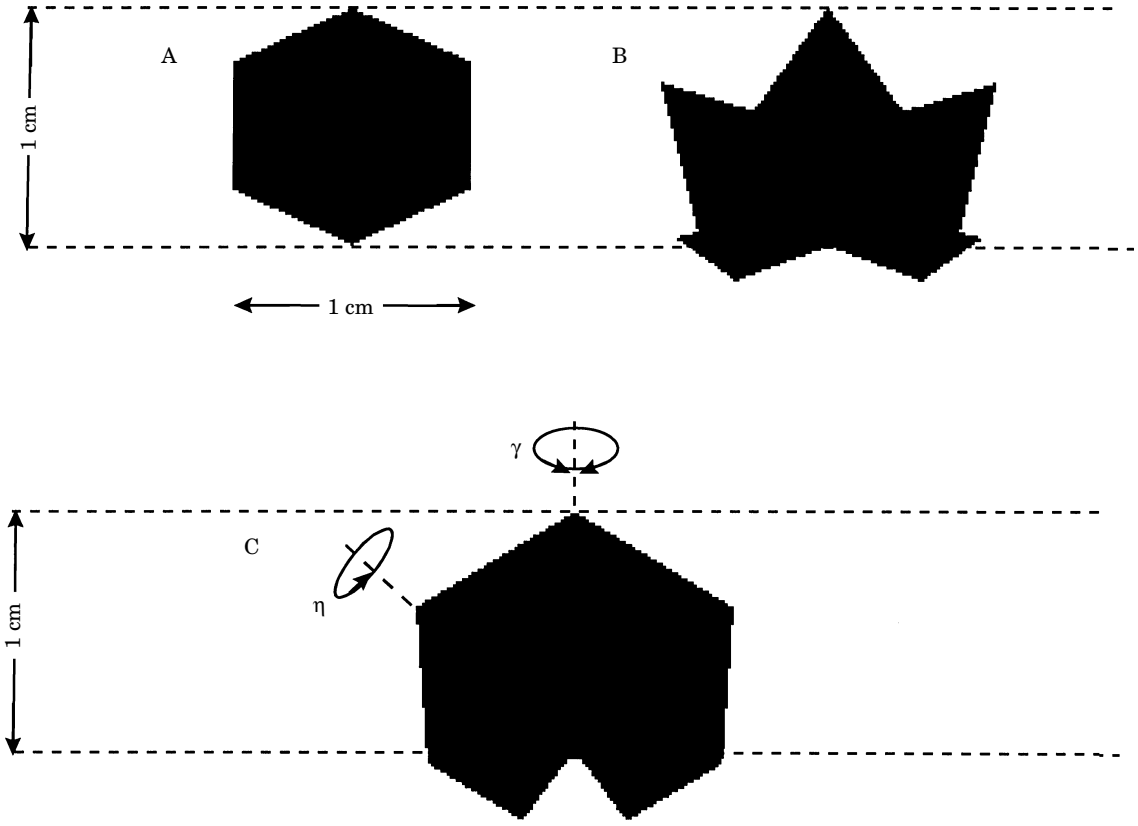

FIG. 2. Prototype of mango (A), cotton (B) and grapevine (C) leaves made of a set of contiguous triangles. Prototype length is 1 cm. Mango leaf prototype width is 1 cm. Rotation angles γ and η around the midrib and the lateral vein, respectively, are used to create 3D leaves of grapevine.

the geometry (i.e. location and direction) of the light sources illuminating the scene, and that of the camera looking at the scene.

The first step was to create a leaf prototype (Fig. 2). In the case of mango, the prototype was a hexagon, the length and width of which were equal to 1. The shape of the hexagon was fitted according to the allometric relationship between blade area and leaf dimensions (Planchais and Sinoquet, 1998). In the case of cotton and grapevine, the prototype was a set of contiguous triangles chosen to fit the leaf shape and allometric relationship between area and length. The length of the two prototypes was also equal to 1. Cotton leaves were flat and defined as 2D objects, while grapevine leaves could be either 2D or 3D, i.e. involute leaves characterized by two rotation angles γ and η around the midrib and the lateral vein, respectively (Fig. 2). Maximum values of angles γ and η observed for the Merlot cultivar were 20 and 30°, respectively (Boursicault, pers. comm.).

The second step consisted of building the vegetation scene, i.e. making a POV-Ray file which integrated the information from digitising, leaf dimensions and attributes. For example, the syntax used to define a mango leaf was as follows:

$$\text{object } \{\text{Prototype scale } \langle L, W, 1\rangle \text{ rotate } \langle \theta, \alpha, \Phi\rangle \text{ translate } \langle x, y, z\rangle \text{ texture } \{\text{Leaf\_type}\}\} \quad (1)$$

A mango leaf was an object of the scene, built from the object Prototype. The prototype object was first scaled in order to match leaf length, leaf width and consequently blade area, since the leaf prototype was defined to verify allometry. The object was then rotated and translated according to the digitising data for leaf orientation and location, respectively. The texture described the optical properties of the leaf, i.e. colour and scattering. Colouring leaves allowed other attributes of the leaf to be coded, e.g. leaf type. The texture instruction also allowed leaves to be made perfect emitters (i.e. luminance not dependent on leaf irradiance or view direction) or perfect diffusers (i.e. luminance linearly related to leaf irradiance).

The last step consisted of defining the light sources and camera. In most applications, a single light source simulating the direct sun beam was used. The light source was then located a large distance from the scene with its direction defined by sun elevation and azimuth. In most applications the camera used an orthographic projection, i.e. a virtual camera using parallel rays to create the image of the scene. Using this type of projection the directional attributes of light interception may be assessed.

Plant image analysis

Virtual photographs created with POV-Ray software were then analysed with image analysis software (Optimas, Imasys, Bothell, Washington, USA). In most applications, image processing consisted of measuring projected leaf area, i.e. counting coloured pixels.

APPLICATIONS

Light interception and partitioning

Figure 3 is an image of a 1-year-old mango plant viewed in the vertical direction. Mango leaves were defined as perfect emitters, with colour defined according to flush number. The number of coloured pixels was, therefore, an estimation of the projected sunlit leaf area (*Ap*) in the view direction. By defining the soil surface area, *As*, occupied by the plant, the ratio *Ap*/*As* was the fraction of light interception in the direction of view. Given the uncertainty in defining *As* in the case of a single plant, we quantified light interception as light interception efficiency (LIE) which is the ratio of projected sunlit leaf area *Ap* to total leaf area *A* (Planchais and Sinoquet, 1998). LIE is also the mean leaf irradiance per unit incident irradiance. Figure 4 shows that LIE decreased with zenith angle, due to rather horizontal leaves. Counting pixels by colour allowed us to estimate the

FIG. 3. Image of a young mango tree viewed in the vertical direction. Violet, blue, green, yellow, orange and red leaves refer to flush number 1 to 6, respectively.

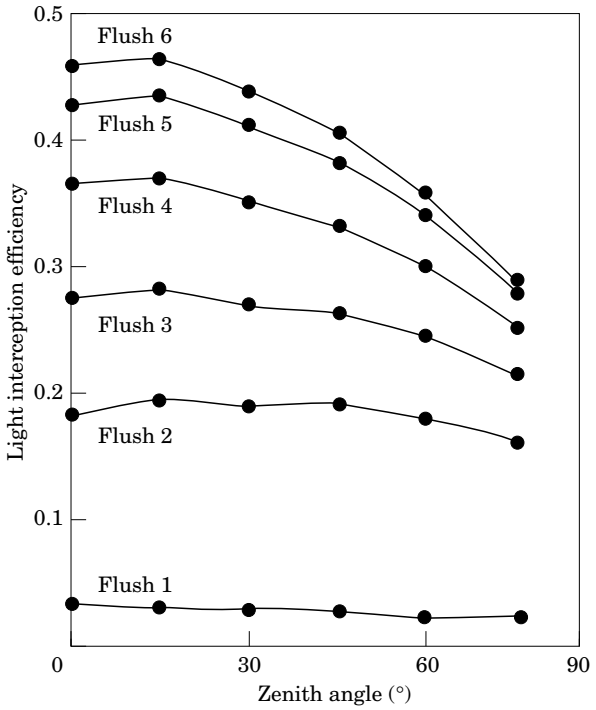

FIG. 4. Light interception of a young mango tree and contribution of each flush to light interception, as a function of zenith angle.

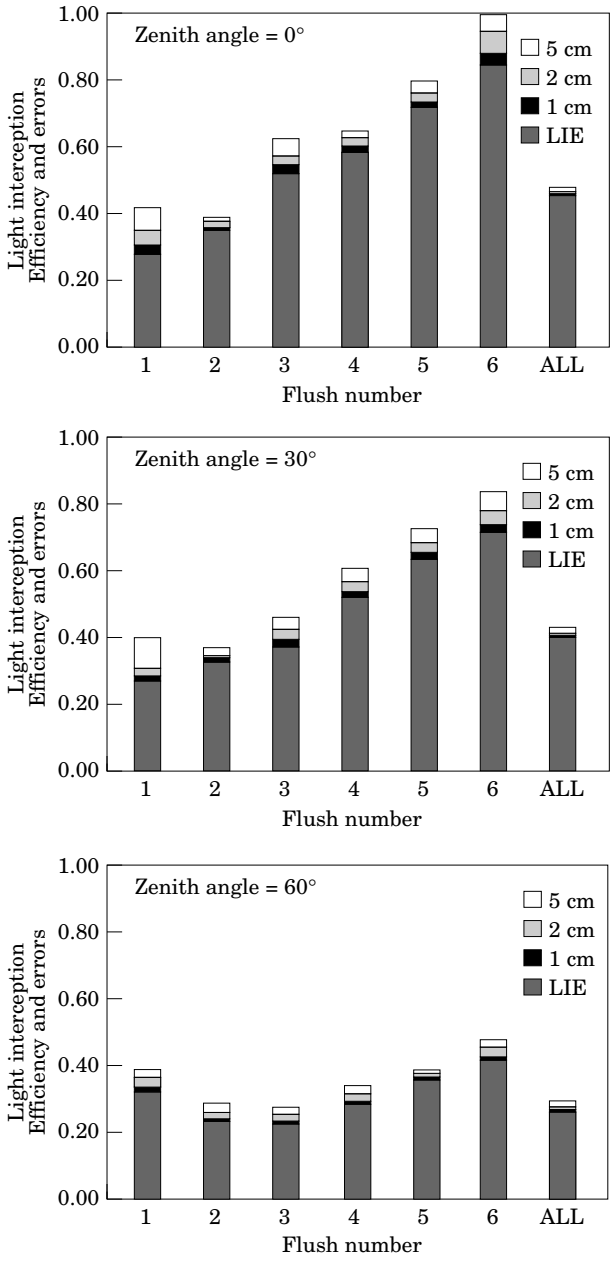

FIG. 5. Light interception efficiency (LIE) at the scale of the flush and the canopy (ALL), and errors in LIE associated with errors in leaf position of ± 1, 2 and 5 cm, for three zenith angles.

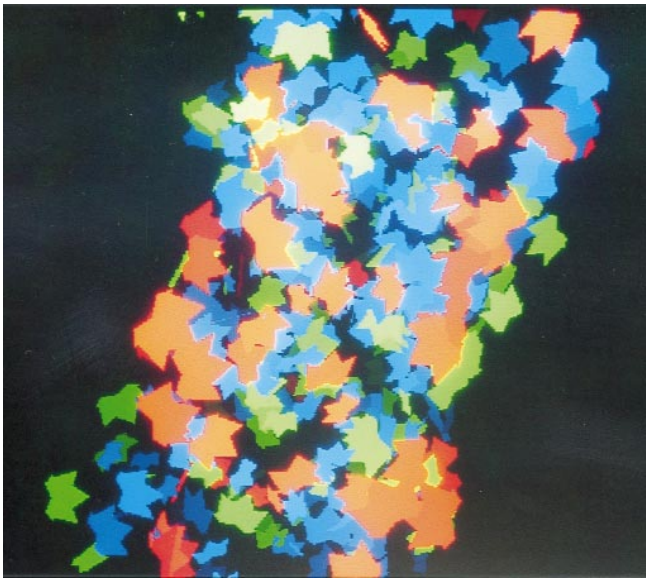

FIG. 6. Image of a cotton canopy seen in the sun direction at noon on the digitising date. Red, green and blue leaves refer to leaves on main stem, vegetative branches and fruiting branches, respectively. Pixel luminance is proportional to leaf altitude within the canopy.

contribution of each flush to LIE, i.e. light partitioning between plant flushes (Fig. 4). For the mango plant, flush number 2 gave the largest contribution to LIE, because of its large leaf area. Looking into LIE at the scale of the flush (Fig. 5) showed that flush LIE increased with flush number, i.e. the older the flush the smaller LIE. As older flushes were generally located below younger ones, this resulted from shading between flushes. The error in LIE associated with the digitising error was quantified by processing images where random errors in spatial co-ordinates (x, y, z) were generated. Sampling error within a uniform probability law in the range $(-E; +E)$ made the mean error of location about 0·6 E. Errors in LIE computed from five 'noisy' images with E = 1, 2 and 5 cm are shown in Fig. 5. At the scale of the flush, the mean error in LIE ranged between 0·01 and 0·03, 0·01 and 0·07, and 0·01 and 0·09, for E = 1, 2 and 5 cm, respectively. However, the maximum error in LIE was 0·03, 0·08 and 0·17, leading to maximum relative errors of 11, 29 and 63 %, for each level of E, respectively. At the scale of the tree, leaf position errors had almost no effect on LIE, even for the largest E of 5 cm.

An image of a cotton row viewed in the direction of the sun at noon on the day the canopy was digitised, i.e. at a zenith angle of 9°, is given in Fig. 6. Red, green and blue colours were attributed to leaves on the main stem, vegetative branches and fruit branches, respectively. Leaves were defined as perfect emitters with luminance proportional to leaf height above the soil surface. For each leaf colour (i.e. red, green, blue), the luminance histogram is therefore an estimation of the vertical profile of sunlit leaf area projected perpendicularly to the sun direction (Fig. 7). Notice that the projected sunlit leaf area per unit of soil surface area is also the fraction of intercepted light. About one third of the leaf area was sunlit. Leaves on the main stem, vegetative branches and fruiting branches contributed 37, 24 and 39 % of light intercepted, respectively. The effect of leaf location errors on the vertical profiles of sunlit area was assessed using noisy images as in the case of mango (Fig. 7). For a maximum error E of ± 2 cm, the mean error (i.e. average of five replications) in projected sunlit leaf area within a 10-cm thick vegetation layer ranged from 2 to 143 cm^2, i.e. a relative error between 4 and 65 %. If E equalled 5 cm, the error ranged from 4 to 188 cm^2, i.e. between 12 and 200 %. The maximum error found in a particular replication was 210 and 440 cm^2, for E = 2 cm and 5 cm, respectively. At the canopy scale, the effect of leaf position errors on light interception estimation was smaller, i.e. 4 and 8 % for E = 2 and 5 cm, respectively.

A virtual fisheye photograph of the grapevine, where the camera looked at the nadir and was located at the top of the fruit zone is given in Fig. 8 A. Leaves were defined as perfect emitters with black and grey tones for primary and lateral leaves, respectively. Analysis of fisheye photographs using the software HEMIPHOT (Steege, 1993) showed that light transmission to the fruit zone in case of Standard Overcast Sky (Moon and Spencer, 1942) was only 3 %. Virtual removal of lateral leaves, i.e. by creating an image with only the primary leaves (Fig. 8 B), increased light transmission to the fruit zone by up to 10 %.

Leaf irradiance distribution

Distribution of irradiance on the leaves can be assessed by defining leaves as perfect diffusers. For such leaves, luminance (normalized between 0 and 1) is equal to the relative leaf irradiance. In order to stimulate the irradiance distribution for direct sunlight (Fig. 9 A), both a light source and a directional camera (i.e. using parallel rays according to the orthographic projection) were positioned in the direction of the sun. In this case, coloured pixels on the picture were the sunlit leaf area. For each coloured pixel, because the single light source was in the same direction as the camera view, the relative irradiance given by the pixel luminance was also $\cos\beta$, i.e. the cosine of the angle β between the leaf normal and the view direction. Moreover, $\cos\beta$ was also the projection coefficient of the leaf area perpendicular to the view direction. Thus, the actual, i.e. non projected, leaf area associated with a pixel of luminance (i.e. leaf irradiance) $\cos\beta$ was exactly the pixel area divided by $\cos\beta$.

For diffuse radiation, incident energy comes from all sky directions. Incident diffuse radiation was therefore approximated by a set of light sources according to the turtle sky, i.e. a sky divided into 46 solid angle sectors allowing for optimal integration properties (Den Dulk, 1989). For diffuse incident radiation, we used the Standard Over Cast (SOC) distribution where sky luminance only depends on elevation (Moon and Spencer, 1942). As in the case of direct irradiance, pixel luminance was equal to leaf irradiance (Fig. 9 B). Leaf irradiance might vary on a single leaf because the number of light sources illuminating any point on a leaf varies. However as light sources were not in the same direction as the camera, pixel luminance did not relate to the projection coefficient of the leaf area associated with the pixel. For this, we had to include information about

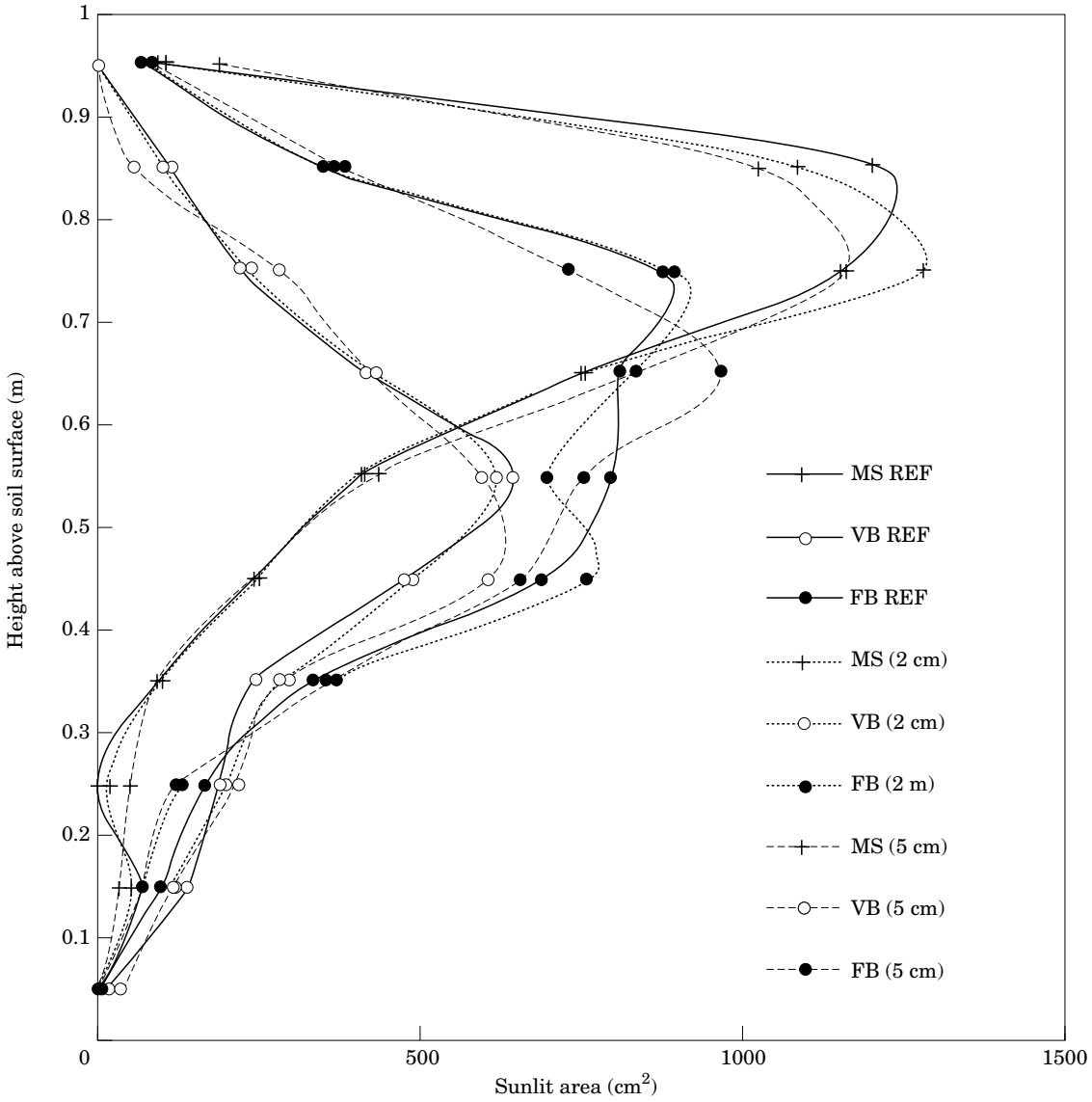

FIG. 7. Vertical profiles of projected area for leaves on main stem (MS), vegetative branches (VB) and fruiting branches (FB), as computed from Fig. 6 (REF) and 'noisy' images with leaf position errors of ± 2 and 5 cm.

$\cos\beta$ from the direct irradiance image (Fig. 9 A). Image processing for deriving leaf irradiance distribution in diffuse sky from the two images (Fig. 9 A and B) was made by a macrocommand written in Optimas.

In case of direct irradiance, a significant amount of the sunlit leaf area had a relative irradiance greater than 1 (Fig. 10 A): because incident radiation referred to the horizontal plane, the maximum irradiance was $1/\sin h$, where h was the sun elevation. When leaves were defined as 2D surfaces, two-thirds of the leaf area had an irradiance greater than 0·8, and mean leaf irradiance of the sunlit area was 0·84. When leaves were defined as 3D objects with angles γ and η of 20 and 30°, respectively, half of the sunlit leaf area had an irradiance greater than 0·8, while mean leaf irradiance decreased to 0·72. In the case of diffuse leaf irradiance (Fig. 10 B), mean irradiance of a sunlit leaf was 0·52 and 0·56, for primary and lateral leaves, respectively, when leaves were defined as flat surfaces. In that case, only 3 and 20 % of primary and lateral leaf area, respectively, had an irradiance above 0·8. In the case of 3D leaves, the mean leaf irradiance was lower, i.e. 0·42 and 0·45 for primary and lateral leaves, respectively. Figure 10 B shows that leaf irradiance distribution of diffuse incident radiation was not uniform, although this is often assumed to be the case in canopy photosynthesis models. Distribution of diffuse irradiance was, however, more uniform in the case of lateral leaves.

The consequences of leaf irradiance on canopy photosynthesis, P_c, can be computed by combining the distribution of leaf irradiance with an equation for the leaf photosynthetic response to light (P_L, μmol CO_2 m^{-2} s^{-1}), for example an exponential model (Daudet and Tchamitchian, 1993)

$$P_L = P_{max}[1 - \exp(-\alpha PAR/P_{max})] \quad (2)$$

where P_{max} is the maximum photosynthetic rate of the leaf

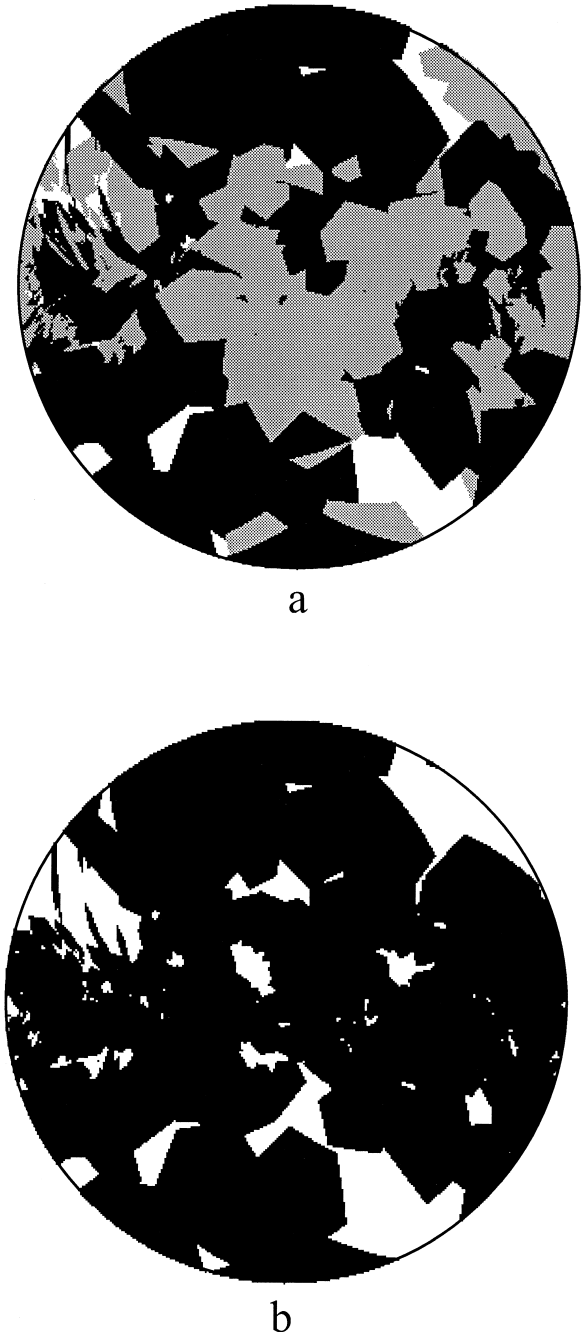

FIG. 8. Fisheye images of the grapevine canopy taken from the top of the fruit zone. Black and grey tones refer to primary and lateral leaves, respectively. A, Canopy with primary and lateral leaves. B, Canopy without lateral leaves.

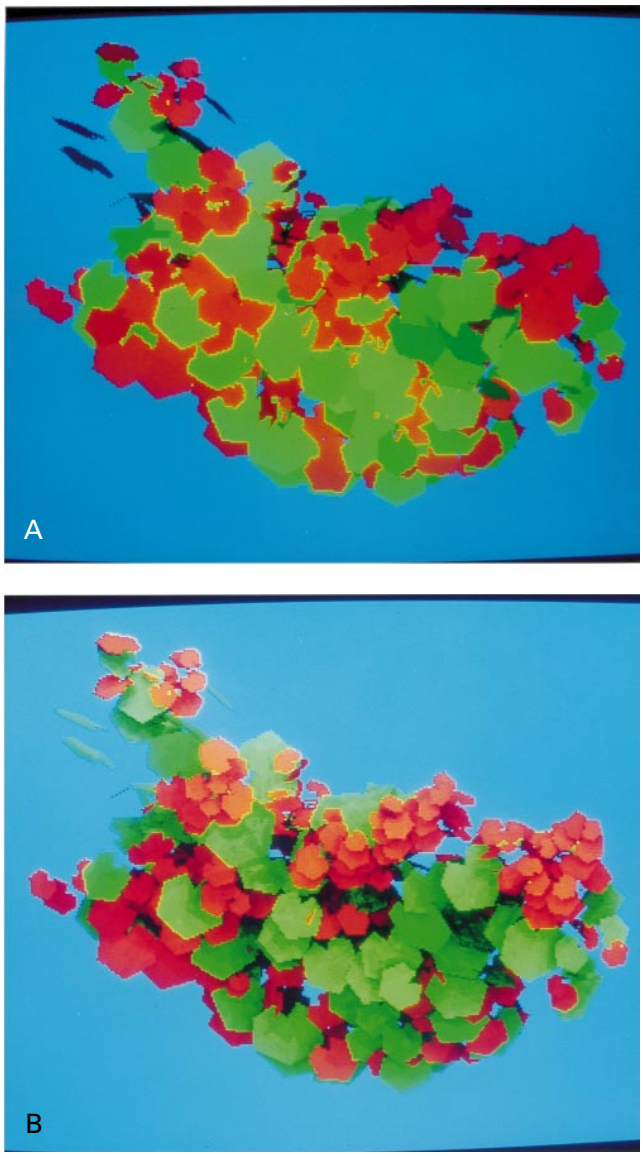

FIG. 9. Image of a grapevine canopy seen in the sun direction at noon on 15 August in Montpellier, France. Green and red leaves refer to primary and lateral leaves, respectively. Leaves are defined as 2D objects ($\gamma = 0°$ and $\eta = 0°$). Pixel luminance refers to leaf irradiance. A, Direct irradiance. B, Diffuse irradiance according to the Standard Overcast Sky.

(μmol CO_2 m^{-2} s^{-1}) at saturating light and α is the quantum yield (μmol CO_2 μmol photons^{-1}). Canopy assimilation P_C (μmol CO_2 s^{-1}) can then be computed as

$$P_C = \sum_{PAR} P_L(PAR)\, A(PAR) \qquad (3)$$

where A(PAR) is leaf area irradiated at a given flux of PAR. P_C was calculated with $\alpha = 0{\cdot}05$ and $P_{max} = 15$ μmol CO_2 m^{-2} s^{-1}, according to values given by During (1988) and Schultz (1995) for different grapevine varieties grown under field conditions. In the case of flat leaves and direct irradiance with 1500 μmol m^{-2} s^{-1} incident PAR, assimilation of the sunlit area of leaves was estimated to be 16·5 μmol CO_2 s^{-1}, primary and lateral leaves contributing 9 and 7·5 μmol CO_2 s^{-1}, respectively. When computed assuming 3D leaves, P_C was 18·2 μmol CO_2 s^{-1}, i.e. an increase of 10 % resulting from a larger sunlit leaf area (+14 %) and a lower photosynthetic rate per unit leaf area (−4 %). By applying the leaf photosynthesis model to the mean foliage irradiance, P_C was overestimated from 4 to 8 %, due to the non-linear response of leaf photosynthesis to light. This highlights the need to take the distribution of leaf irradiance into account when calculating canopy photosynthesis.

Otherwise, computing P_c for a virtual canopy made of primary leaves only showed that the marginal contribution of lateral leaves to carbon acquisition was +16%, due to a larger sunlit area in the actual canopy (+9%) and better carbon gain per unit sunlit area (+7%). Notice that the marginal contribution of lateral leaves to carbon gain is probably underestimated as lateral leaves have been reported to show larger photosynthetic capacities than primary leaves (Hirano *et al.*, 1994). Although these calculations only aimed to exemplify the methods, one can see the dilemma lateral leaves present for grapevine management; grape quality is mainly determined by fruit irradiance and assimilate supply (Jackson and Lombard, 1993), and the effects of lateral leaves on these two features are negative and positive, respectively.

DISCUSSION

Computing light attributes from plant models or plant images has been proposed by several authors: light interception by soybean (Meyer *et al.*, 1984), cactus plants *Opuntia ficus-indica* L. (Garcia de Cortazar, Acevedo and Nobel, 1985), poplar trees (Chen *et al.*, 1993) or theoretical tree shoots (Takenaka, 1994); penumbra effects in a canopy made of elliptic leaves (Myneni and Impens, 1985); and canopy reflectance computed from ray-tracing techniques in plants made of elliptic leaves attached to a vertical stem (Ross and Marshak, 1988). In comparison with previous studies, the method reported here shows two main differences. Firstly the method deals with actual plants, due to the use of the 3D digitising technique, while other methods deal with theoretical plants which can be parameterised for a given species (e.g. poplar, Chen *et al.*, 1993) or not. This feature may be important with regard to light interception because the actual distribution of foliage in space may be quite different from the theoretical distribution based on simple rules of phyllotaxy (Drouet and Moulia, 1998). This is especially true for cotton, where diurnal changes in leaf orientation, i.e. heliotropism, strongly affect its ability to capture light (Lang, 1973; Thanisawanyangkura *et al.*, 1997). Secondly the reported method uses image processing software to both synthesise virtual photographs and to compute attributes of light interception. Creating images of virtual plants has been previously proposed by several authors (e.g. de Reffye *et al.*, 1988; Prusinkiewicz and Lindenmayer, 1990; Room *et al.*, 1996). On the other hand, Andrieu and Sinoquet (1993) derived gap fractions by image analysis of actual photographs of artificial plants made of green tissue planted on red-painted soil. In the present method, image synthesis and image analysis were combined to derive light interception properties. Image synthesis software has to work so that the number of pixels representing any object fits its projected area. This is the case for POV-Ray, but other image synthesis software systematically overestimates the projected areas (see Aries, Prévot and Monestiez, 1993). Virtual optical properties are attributed to leaves. This allows one to compute not only light interception at the canopy level [i.e. by distinguishing soil and vegetation as proposed by Andrieu and Sinoquet (1993)] but also light partitioning between the canopy components. In this paper we applied this method to distinguish light interception by three classes of cotton leaves. However, a number of other applications may be found, especially to evaluate light competition in intercropping systems. This is all the more important because there is no satisfactory method based on light sensors or actual photographs to derive light partitioning between several species grown on the same land unit (Sinoquet and Caldwell, 1995). As shown in Fig. 4, the method also allows computation of vertical profiles of light interception in the canopy. Other methods for this purpose involve radiance measurements (Andrieu and Ivanov, 1993), stereo photographs (Ivanov *et al.*, 1995), or laser telemetry (Sinoquet *et al.*, 1993). The first two of these allow a foliage element to be located in the canopy if it is seen on two photographs taken from two different directions of view. Leaves seen on only one photograph cannot be included in the analysis; this biases the resulting light interception profile. The third method measures the spatial location of interception of beams sent by a laser distance meter, i.e. requires complex and expensive equipment.

The method reported here also has limitations. The first concerns making plant images. Firstly, the accuracy for locating a point in space with the digitiser is about 1 cm in field conditions (Thanisawanyangkura *et al.*, 1997). It may be worse in windy conditions or in dense canopies where the operator may accidentally change leaf positions. The effect of digitising accuracy on the estimation of light microclimate was assessed by creating noisy images. Random errors of some centimetres in leaf position had no influence on light computations at the canopy scale, but did have a significant effect on light attributes computed at the intra-canopy scale, i.e. light interception at the flush scale in mango (Fig. 5) and vertical profiles of light interception in cotton (Fig. 7). Extrapolating this tendency suggests that the smaller the spatial scale the larger the uncertainty in light estimation: this probably prevents application of this type of method for computing light attributes at the leaf scale. In any case, the application of this method should include assessment of the accuracy of calculation. For this purpose, using noisy images saves time in comparison with replication of digitising measurements. Secondly, leaves are more easily defined as 2D objects. This assumption affects the distribution of leaf angles, and thus projected leaf areas and the leaf irradiance distributions (Fig. 10). The quantitative effect of assuming flat leaves was assessed by defining 3D leaves when making the grapevine plant images. As the leaf prototype is a set of triangles, 3D leaves may be defined in software POV-Ray. Thirdly, the canopy is assumed not to move, yet wind causes the leaf position to vary. This mainly affects the leaf irradiance distribution. However, although the effect of leaf fluttering on leaf irradiance fluctuations and leaf photosynthesis has been investigated (Pearcy, Roden and Gamon, 1990), the effect at the canopy level is not documented.

The second type of limitation for the proposed method concerns light calculations. The method is very effective for light properties related to a single direction. This is especially the case for directional light interception and partitioning, because synthesis of the plant image is fast and image

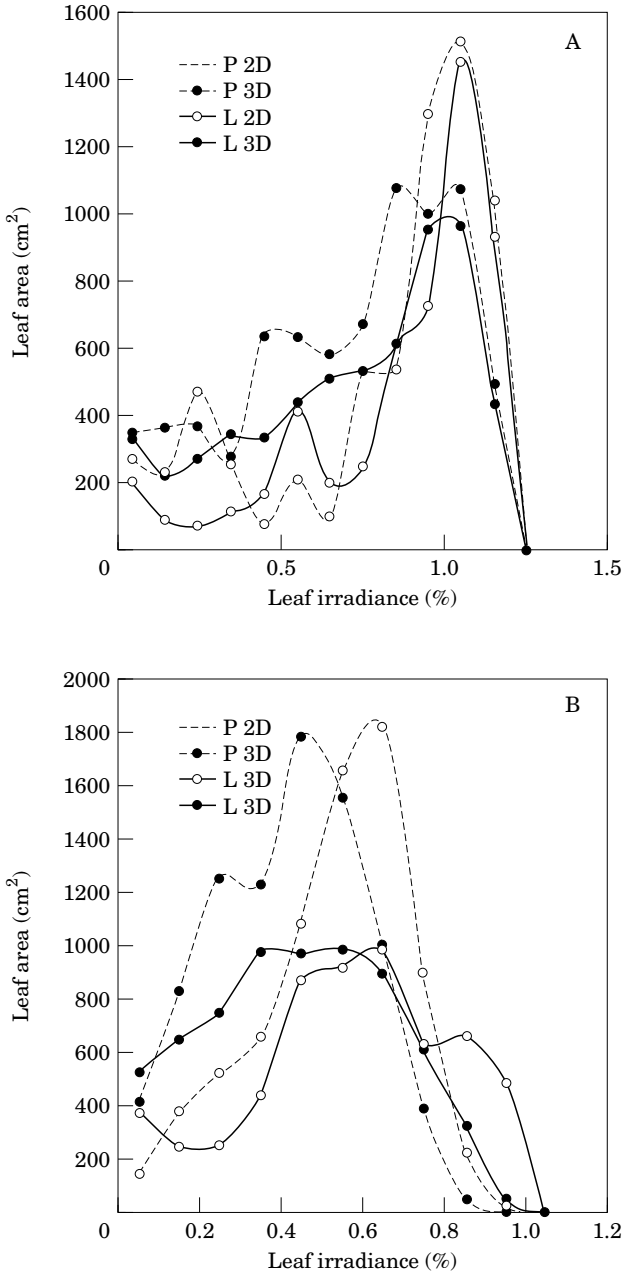

FIG. 10. Leaf irradiance distribution on the sunlit foliage of a grapevine canopy, for primary (P) and lateral (L) leaves defined as 2D or 3D objects. A, Direct irradiance. B, Diffuse irradiance according to the Standard Overcast Sky.

analysis (i.e. counting coloured pixels) is easy. Computing leaf irradiance in the case of diffuse sky is much less attractive. On the one hand, making the plant picture is time-consuming: on a Pentium 133 computer, it takes about 2 h for a canopy made of some hundreds of leaves where the diffuse sky is defined as a set of 46 light sources. On the other hand, image analysis to derive the leaf irradiance distribution is cumbersome, and not feasible with simple software. Another limitation is that the method does not deal with light scattering. In particular it is impossible to derive canopy reflectance data. Finally this method is very well suited for computing light interception in the case of plants with a small number of leaves, e.g. the mango tree (Fig. 3). Indeed digitising and image synthesis are fast, and are particularly useful as classical light models (i.e. based on Beer's law) do not work for such canopies. Notice also that the same methods for light computations could be used with simulations of plant morphogenesis so that light attributes could be computed for various stages of plant development and various modifications of plant architecture such as altered lengths and angles of plant parts.

ACKNOWLEDGEMENTS

We are grateful to the POV-Ray team co-ordinated by C. Young (e-mail: 76702.1655@compuserve.com) for POV-Ray freeware, and Dr P. Room for helpful comments on the manuscript.

LITERATURE CITED

Andrieu B, Ivanov N. 1993. Use of radiance measurements to assess the position of phytoelements in a vegetation canopy. *Agricultural and Forest Meteorology* **66**: 139–157.

Andrieu B, Sinoquet H. 1993. Evaluation of structure description requirements for predicting gap fraction of vegetation canopies. *Agricultural and Forest Meteorology* **65**: 207–227.

Aries F, Prévot L, Monestiez P. 1993. Geometrical canopy modelling in radiation simulation studies. In: Varlet-Grancher C, Bonhomme R, Sinoquet H, eds. *Crop structure and light microclimate: characterization and applications*. Paris: INRA Editions, 159–173.

Buwalda JG, Curtis JP, Smith GS. 1993. Use of interactive computer graphics for simulation of radiation interception and photosynthesis for canopies of kiwifruit vines with heterogeneous surface shape and leaf area distribution. *Annals of Botany* **72**: 17–26.

Chen SG, Impens I, Ceulemans R, Kockelbergh F. 1993. Measurement of gap fraction of fractal generated canopies using digitalized image analysis. *Agricultural and Forest Meteorology* **65**: 245–259.

Daudet FA, Tchamitchian M. 1993. Radiative exchange and photosynthesis. In: Varlet-Grancher C, Bonhomme R, Sinoquet H, eds. *Crop structure and light microclimate: characterization and applications*. Paris: INRA Editions, 401–417.

De Reffye P, Edelin C, Françon J, Jaegger M, Puech C. 1988. Plant models faithful to botanical structure and development. *Computer Graphics* **22**: 151–158.

Den Dulk JA. 1989. *The interpretation of remote sensing, a feasibility study*. PhD Thesis, Wageningen.

Drouet JL, Moulia B. 1998. Spatial re-orientation of maize leaves affected by initial plant orientation and density. *Agricultural and Forest Meteorology* **88**: 85–100.

During H. 1988. CO_2 assimilation and photorespiration of grapevine leaves: responses to light and drought. *Vitis* **27**: 199–208.

Garcia de Cortazar V, Acevedo E, Nobel PS. 1985. Modeling of PAR interception and productivity by *Opuntia ficus-indica*. *Agricultural and Forest Meteorology* **34**: 145–162.

Gutschick VP, Barron MH, Waechter DA, Wolf MA. 1985. Portable monitor for solar radiation that accumulates irradiance histograms for 32 leaf-mounted sensors. *Agricultural and Forest Meteorology* **33**: 281–290.

Hirano K, Noda M, Haegawa S, Okamoto G. 1994. Contribution of lateral and primary leaves to the development and quality of Kyoho grape berry. *Journal of the Japanese Society of Horticultural Science* **63**: 515–521.

Ivanov N, Boissard P, Chapron M, Andrieu B. 1995. Computer stereo plotting for 3-D reconstruction of a maize canopy. *Agricultural and Forest Meteorology* **75**: 85–102.

Jackson DI, Lombard PB. 1993. Environmental and management practices affecting grape composition and wine quality—A review. *American Journal of Enology and Viticulture* **44**: 409–430.

Lang ARG. 1973. Leaf orientation of a cotton plant. *Agricultural Meteorology* **11**: 37–51.

Meyer GE, Davison D, Lamb JA, Splinter WJ. 1984. Crop simulation studies using 3-D graphics: canopy architecture and light interception. Paper ASAE NO 84-4013, St Joseph, Michigan, 24 p.

Moon P, Spencer DE. 1942. Illumination from a non-uniform sky. *Transactions of the Illumination Engineering Society* **37**: 707–726.

Moulia B, Sinoquet H. 1993. Three-dimensional digitizing systems for plant canopy geometrical structure: a review. In: Varlet-Grancher C, Bonhomme R, Sinoquet H, eds. *Crop structure and light microclimate: characterization and applications*. Paris: INRA Editions, 183–193.

Myneni RB, Impens I. 1985. A procedural approach for studying the radiation regime of infinite and truncated foliage spaces. I. Theoretical considerations. *Agricultural and Forest Meteorology* **33**: 323–337.

Pearcy RW, Roden JS, Gamon JA. 1990. Sunfleck dynamics in relation to canopy structure in a soybean (*Glycine max* L. Merr.) canopy. *Agricultural and Forest Meteorology* **52**: 359–372.

Planchais I, Sinoquet H. 1998. Foliage determinants of light interception in sunny and shaded branches of Fagus sylvatica (L.). *Agricultural and Forest Meteorology* **89**: 241–253.

Polhemus Inc. 1993. *3SPACE FASTRAK User's Manual*, *Revision F*. Colchester, VT, USA: Polhemus Inc.

Prusinkiewicz P, Lindenmayer A. 1990. *The algorithmic beauty of plants*. New York: Springer-Verlag.

Raab FH, Blood EB, Steiner TO, Jones HR. 1979. Magnetic position and orientation tracking system. *IEEE Transactions of Aerospace and Electronic Systems* **15**: 709–718.

Roden JS, Pearcy RW. 1993. Effect of leaf flutter on the light environment of poplars. *Oecologia* **93**: 201–207.

Room PM, Hanan JS, Prusinkiewicz P. 1996. Virtual plants: new perspectives for ecologists, pathologists and agricultural scientists. *Trends in Plant Science* **1**: 33–38.

Ross JK. 1981. *The radiation regime and the architecture of plant stands*. The Hague: Junk W. Pubs.

Ross JK, Marshak AL. 1988. Calculation of canopy bidirectional reflectance using the Monte Carlo method. *Remote Sensing of Environment* **24**: 213–225.

Schultz HR. 1995. Photosynthesis of sun and shade leaves of field-grown grapevine in relation to leaf age. Suitability of the plastochron concept for the expression of physiological age. *Vitis* **32**: 197–205.

Sinoquet H, Caldwell RM. 1995. Estimation of light capture and partitioning in intercropping systems. In: Sinoquet H, Cruz P, eds. *Ecophysiology of tropical intercropping*. Paris: INRA Editions, 79–97.

Sinoquet H, Rivet P. 1997. Measurement and visualisation of the architecture of an adult tree based on a three-dimensional digitising device. *Trees* **11**: 265–270.

Sinoquet H, Moulia B, Bonhomme R. 1991. Estimating the three-dimensional geometry of a maize crop as an input of radiation models: comparison between three-dimensional digitising and plant profiles. *Agricultural and Forest Meteorology* **55**: 233–249.

Sinoquet H, Valmorin M, Cabo X, Bonhomme R. 1993. DALI: an automated laser distance meter system for measuring profiles of vegetation. *Agricultural and Forest Meteorology* **67**: 43–64.

Sinoquet H, Adam B, Rivet P, Godin C. 1997. Interactions between light and plant architecture in an agroforestry walnut tree. *Agroforestry Forum* **8**: 37–40.

Smith GS, Curtis JP. 1995. A fast and effective method of measuring tree structure in 3 dimensions. In: Habib R, Blaise P, eds. *Proceedings of the 4th International Symposium on Computer Modelling in Fruit Research and Orchard Management*, Avignon, September 4–8, 1995. Avignon: INRA-ISHS, 15–20.

Steege H ter. 1993. *HEMIPHOT: a programme to analyse vegetation indices, light and light quality from hemispherical photographs*. Wageningen: The Tropenbos Foundation.

Takenaka A. 1994. Effects of leaf blade narrowness and petiole length on the light capture efficiency of a shoot. *Ecological Research* **9**: 109–114.

Thanisawanyangkura S, Sinoquet H, Rivet P, Crétenet M, Jallas E. 1997. Leaf orientation and sunlit leaf area distribution in cotton. *Agricultural and Forest Meteorology* **86**: 1–15.